Title
Embryonic AP1 Transcription Factor Deficiency Causes a Collodion Baby-Like Phenotype

Journal
Journal of Investigative Dermatology, 137(9)

ISSN
0022-202X

Authors
Young, Christina A
Eckert, Richard L
Adhikary, Gautam
et al.

Publication Date
2017-09-01

DOI
10.1016/j.jid.2017.04.032

Peer reviewed

HHS Public Access

Author manuscript

J Invest Dermatol. Author manuscript; available in PMC 2017 September 01.

Published in final edited form as:

J Invest Dermatol. 2017 September ; 137(9): 1868–1877. doi:10.1016/j.jid.2017.04.032.

EMBRYONIC AP1 TRANSCRIPTION FACTOR DEFICIENCY CAUSES A COLLODION BABY-LIKE PHENOTYPE

Christina A. Young[1], **Richard L. Eckert**[1,2,3,4], **Gautam Adhikary**[1], **Debra Crumrine**[6], **Peter M. Elias**[6], **Miroslav Blumenberg**[7], and **Ellen A. Rorke**[5]

[1]Department of Biochemistry and Molecular Biology, University of Maryland School of Medicine, Baltimore, Maryland [2]Department of Dermatology, University of Maryland School of Medicine, Baltimore, Maryland [3]Department of Reproductive Biology, University of Maryland School of Medicine, Baltimore, Maryland [4]Marlene and Stewart Greenebaum Cancer Center, University of Maryland School of Medicine, Baltimore, Maryland [5]Department of Microbiology and Immunology, University of Maryland School of Medicine, Baltimore, Maryland [6]Dermatology Service, Veterans Affairs Medical Center, San Francisco and Department of Dermatology, University of California, San Francisco, California [7]The R.O. Perelman Department of Dermatology, Department of Biochemistry and Molecular Pharmacology, New York University Langone Medical Center, New York, New York

Abstract

AP1 transcription factors are important controllers of gene expression in the epidermis, and altered AP1 factor function can perturb keratinocyte proliferation and differentiation. However, our understanding of how AP1 signaling changes may underlie or exacerbate skin disease is limited. We have shown that inhibiting AP1 factor function in suprabasal adult epidermis leads to reduced filaggrin levels and to a phenotype that resembles the genetic disorder, ichthyosis vulgaris. We now show that inhibiting AP1 factor function during development in embryonic epidermis produces marked phenotypic changes including reduced filaggrin mRNA and protein levels, compromised barrier function, marked ultrastructural change and enhanced dehydration susceptibility that resembles the phenotype observed in the flaky tail mouse, a model for ichthyosis vulgaris. In addition, the AP1 factor-deficient newborn mice also display a collodion membrane phenotype which is not observed in flaky tail mice or in newborn individuals with ichthyosis vulgaris, but is present in other forms of ichthyosis. This mixed phenotype suggests that a need for a better understanding of the possible role of filaggrin loss and AP1 transcription factor deficiency in ichthyoses and collodion membrane formation.

Correspondence Richard L. Eckert, Ph.D., John F.B. Weaver Distinguished Professor, Chair - Department of Biochemistry and Molecular Biology, Associate Director - Basic Sciences Greenebaum Cancer Center, University of Maryland School of Medicine, 108 North Greene Street, Rm 103, Baltimore, Maryland 21201, Ph: 410-706-3220, reckert@umaryland.edu.

Conflict of Interest

The authors declare no conflict of interest

Keywords

TAM67; AP1; jun; fos; loricrin keratoderma; hyperkeratosis; epidermis; keratins; embryonic development; skin development; filaggrin; ichthyosis; ichthyosis vulgaris; collodion baby; cornification

Introduction

AP1 transcription factors comprise a family of proteins, including c-jun, junB, junD, c-fos and Fra-1 (Angel et al., 2001; Eckert et al., 1997), which form homo- and heterodimers that bind to specific DNA response elements in regulatory regions of target genes to drive transcription (Angel et al., 2001; Eckert et al., 1997). AP1 factors in the epidermis are expressed in a differentiation-dependent manner (Welter and Eckert, 1995) and control expression of differentiation associated genes (Crish et al., 1998; Crish et al., 2006), including filaggrin (Jang et al., 1996). We recently described a phenotype in adult mice that includes epidermal hyperproliferation, parakeratosis, hyperkeratosis, impaired barrier function, nuclear loricrin accumulation and reduced filaggrin level in response to suprabasal epidermis-specific inactivation of activator protein 1 (AP1) transcription factor function (Rorke et al., 2010; Rorke et al., 2015a; Rorke et al., 2015b). In addition, we observe nuclear loricrin accumulation and, in some animals, constricting bands (pseudoainhum) encircle the tail and digits (Rorke et al., 2015b).

We now show that epidermis-specific inactivation of AP1 factor function during embryonic development causes reduced filaggrin mRNA and protein levels, compromised barrier function and abnormal epidermal ultrastructure which mimic the phenotype observed in the flaky tail mouse model of ichthyosis vulgaris and the phenotype of the corresponding human disease (Smith et al., 2006; Presland et al., 2000). However, we also observe nuclear loricrin accumulation and a collodion baby-like phenotype, which is not observed in ichthyosis vulgaris but is a feature of other ichthyosis types including loricrin keratoderma, lamellar ichthyosis and congenital ichthyosiform erythroderma (Oji et al., 2010). These findings suggest that loss of AP1 factor signaling in the suprabasal epidermis in adult mice is sufficient to cause a phenotype that shares properties of ichthyosis vulgaris (epidermal scaling, etc., filaggrin loss) (Presland et al., 2000) and loricrin keratoderma (nuclear loricrin localization, collodion phenotype) (Matsumoto et al., 2001; Yeh et al., 2013). These findings suggest that reduced filaggrin levels in AP1 factor-deficient mice is associated with a complex phenotype, and point to the need to better understand the potential role of AP1 factor deficiency in the development of ichthyotic disease.

Results

Role of AP1 transcription factors in the embryonic epidermis

In the present study, we examined the impact of *in utero* AP1 factor inactivation in suprabasal embryonic epidermis. We mated heterozygous (TAM67+/−) and heterozygous (rTA+/−) mice to generate control (TAM67-/rTA−, TAM67+/rTA−, TAM67-/rTA+) and TAM67-rTA (TAM67+/rTA+) embryos. We then treated the pregnant dams with 2 mg/ml

doxycycline beginning at E13.5, E15.5 and E17.5 and harvested embryos at E20 (Fig. 1A). As anticipated, doxycycline treatment induces TAM67-FLAG expression in TAM67+/rTA+ embryos, but not in non-transgenic (control) embryos (Fig. 1B). To examine the impact on phenotype, we initiated doxycycline treatment on E13.5, E15.5 and E17.5, and permitted the mice to be born. Fig. 1C shows mouse images at 12 h post-birth. E13.5 and E15.5 TAM67-rTA mice display a collodion baby-like phenotype, which is not evident in the E17.5 mice. The phenotype was present in one hundred percent of E13.5 and E15.5 TAM67-positive mice, all of which died within 24 h after birth.

We next characterized the effect of AP1 factor inactivation on epidermal histology. Fig. 2A shows that doxycycline-treated control mice display normal epidermal development which includes formation of a well-structured barrier (arrows). In contrast, in doxycycline-treated TAM67-rTA mice, the epidermis is thicker and the epidermal surface is less-structured. These changes are particularly apparent when treatment is initiated on E13.5 or E15.5. Initiating treatment on E17.5 produces a less perturbed epidermis with a more normal appearing surface. To assess the impact of TAM67 expression on barrier function, E13.5, E15.5 and E17.5 embryos were harvested on E20 and challenged with toluidine blue. Fig. 2B shows that the E13.5 and E15.5 mice have reduced barrier function, but that the E17.5 mice retain barrier function. We next boiled equal-sized samples of epidermis under reducing and denaturing conditions to prepare cornified envelopes. Control mice yield many envelopes, while very few are detected in E13.5 or E15.5 mice, and intermediate numbers in E17.5 mice (Fig. 2C/D). It is likely that the reduction in envelope number is due to formation of thin envelopes that are not resistant to boiling in detergent and reduction agent (Robinson et al., 1996; Robinson et al., 1997). As will be discussed later, this is consistent with ultrastructure findings showing a reduction in envelope thickness.

Expression of epidermal markers

Similar to adult epidermis (Rorke et al., 2015b; Rorke et al., 2015a), TAM67-FLAG localizes in the nucleus of suprabasal epidermal keratinocytes in doxycycline-treated TAM67-rTA embryos (Fig. 3A). Fig. 3B shows that suprabasal TAM67 expression does not alter involucrin distribution (green stain). PCNA is present in proliferating cells in the basal epidermis in all samples (red stain) (Fig. 3B), although staining is generally less in control epidermis. Keratin 14 is a basal epidermal layer marker which displays little change in tissue distribution (Fig. 3C). Loricrin redistributes from a membrane location in control epidermis to inside the nucleus in TAM67-FLAG expressing epidermis (Fig. 3D). This is also observed in TAM67-positive adult mouse epidermis (Rorke et al., 2015b; Rorke et al., 2015a). Fig. 3E shows that the overall levels of K10, K14, involucrin and loricrin are not markedly altered in TAM67-expressing epidermis. To confirm loricrin nuclear translocation, we cultured murine keratinocytes derived from wild-type and TAM67-rTA mice in doxycycline-containing medium. In wild-type keratinocytes loricrin localizes in punctate foci throughout the cell and surrounding the nucleus (Fig. 4A). In contrast, loricrin localizes in the nucleus in TAM67-FLAG expressing cells (Fig. 4A). Fig. 4B shows that TAM67 expression does not markedly alter K10, K6, loricrin or involucrin level in cultured murine keratinocytes.

Filaggrin expression

Filaggrin is a key protein involved in cornified envelope assembly and barrier formation (Dale et al., 1985; Irvine et al., 2011; Ishida-Yamamoto et al., 1999) and filaggrin loss-of-function and reduced level is observed in human ichthyosis vulgaris (McLean, 2016; Smith et al., 2006; Oji et al., 2010). Fig. 4C shows that filaggrin and profilaggrin levels are markedly reduced in TAM67-positive embryonic epidermis. Immunostaining (Fig. 4D) confirms the reduction and reveals residual staining confined to punctate locations in the epidermis. RT-PCR analysis shows that the loss of filaggrin protein is associated with loss of filaggrin mRNA (Fig. 4E) and that filaggrin 2 encoding mRNA is also reduced (Fig. 4E).

Ultrastructure of TAM67-expressing embryonic epidermis

Induction of TAM67 expression in embryonic epidermis at E13.5 or E15.5 results in loss of epidermal barrier function, but this is not observed in E17.5 epidermis (Fig. 2). This suggests that 2.5 d of exposure to TAM67 is not sufficient to induce changes in epidermal structure sufficient to compromise the barrier. However, we were concerned that this tissue may display ultrastructural changes, since we observe biochemical and cellular changes in the E17.5 epidermis (Fig. 3D and Fig. 4C). To examine epidermal ultrastructure, pregnant dams were treated with doxycycline beginning at the indicated embryonic day and epidermal tissue was processed at E20 for ultrastructural analysis. Analysis shows that cornified envelope thickness is significantly reduced in TAM67-positive E13.5, E15.5 and E17.5 epidermis (Fig. 4F). As shown in Fig. 5, control epidermis displays a well-structured stratum corneum with normal secretion of granule contents at the stratum granulosum (SG)/stratum corneum (SC) junction (white arrows, upper panel), and the presence of well-formed and abundant keratohyalin granules (K, lower panel). The extracellular lamellar bilayers are regular (upper insert), the cornified envelopes are thick and dense (middle insert) and abundant lamellar bodies are present (lower insert). In contrast, reduced-thickness cornified envelopes are observed in E13.5, E15.5 and E17.5 epidermis (black double arrows). In addition, keratohyalin granule (K) number is reduced, and morphology of cornified layer (e.g., E17.5, left insert) is abnormal. In general, the most severe ultrastructure changes are observed in epidermis from E13.5 and E15.5 mice.

Gene array analysis

We next used gene array to compare mRNA expression in TAM67-negative and positive embryonic skin. Table 1 lists a collection of genes that are differentially expressed. TAM67-negative embryonic epidermis, which differentiates normally, is enriched in mRNA encoding cutaneous and hair keratins, hair keratin-associated proteins and late cornified envelope precursors. Filaggrin related genes, including filaggrin family member 2 and hornerin, are also enriched. In contrast, TAM67-positive embryonic skin is enriched in the proliferation associated keratins (Krt6a, Krt6b, Krt16), early envelope precursors, including the small proline-rich proteins, various proteases and proteasome inhibitors, and defensin family members.

Discussion

The AP1 factor-deficiency phenotype

We inactivated suprabasal AP1 factor function in embryonic epidermis at embryonic day E13.5, E15.5 and E17.5 and monitored for changes at E20 and post-birth. When TAM67 expression is induced at E13.5 and E15.5, all TAM67-expressing mice are born encased in a collodion membrane. Histology of TAM67-positive E20 embryos reveals a thickened epidermis and a malformed epidermal cornified layer. The cornified layer appears fragile and not tightly tethered to the underlying tissue. This phenotype is associated with a 95% reduction in cornified envelope formation and loss of barrier function. Envelope formation was measured by boiling equivalent skin samples in detergent and reducing agent. Since only well-formed envelopes survive this process (Robinson et al., 1996; Robinson et al., 1997), our finding suggest that the envelopes formed in TAM67-positive epidermis are fragile. In addition, the TAM67-positive embryos are born bloated, presumably due to abnormal fluid uptake in utero, and rapidly and visibly dehydrate following air exposure. This phenotype was associated with prominent ultrastructural changes. The most prominent include a reduction in keratohyalin granule number and the presence of thinner cornified envelopes.

In contrast, initiation of TAM67 expression at E17.5 produces mice that appear normal at birth and have normal epidermal barrier function. However, there are signs of abnormalities, as cornified envelope number is reduced by 65%, filaggrin protein and mRNA levels are reduced, and there are clear changes in epidermal ultrastructure including reduced keratohyalin granule number and thinner cornified envelopes. However, the ultrastructural changes are not as severe as those observed in E13.5 and E15.5 epidermis. Thus, it appears that disease severity progresses with the length of time that AP1 factor function is inactivated in utero. The 2.5 day period of AP1 factor inactivation in the E17.5 mice provides adequate time to initiate phenotype development but is not enough time to induce the enhanced dye permeability or collodion phenotype.

Immunostaining suggests minimal alteration in expression of some differentiation marker proteins (Fig. 3). However, array analysis identifies differentiation-associated changes in gene expression consistent with a shift towards enhanced proliferation and reduced differentiation. Messenger RNA encoding cutaneous and hair keratins, hair keratin-associated proteins, late cornified envelope precursors and filaggrin gene family members are enriched in TAM67-negative (control) epidermis. TAM67-positive embryonic skin is enriched in the proliferation associated keratins (Krt6a, Krt6b, Krt16), early envelope precursors, various proteases and proteasome inhibitors, defensin family members, and repetin. Thus, the array data suggests that TAM67 expression reduces differentiation and enhances proliferation.

AP1 transcription factor loss and phenotype development We show that inactivation of AP1 transcription factor function in the suprabasal epidermis creates an ichthyosis vulgaris-like phenotype; however, there is no previous evidence that AP1 transcription factors have a role in this disease. Thus, it is important to understand how perturbing epidermal AP1 factor function may cause this phenotype. An important place to start is the impact of AP1 factor

inactivation on expression/function of AP1 factor target proteins. Two such targets, loricrin and filaggrin, are implicated in the genesis of ichthyotic disease (Korge et al., 1997; Maestrini et al., 1996; O'Driscoll et al., 2002; Smith et al., 2006; McLean, 2016; Presland et al., 2000).

Filaggrin is a structural protein that is produced as a large precursor called profilaggrin that is the major constituent of keratohyalin granules (Sandilands et al., 2009). Profilaggrin is dephosphorylated and proteolyzed into filaggrin monomers and these monomers bind to and bundle keratin intermediate filaments (Irvine, 2007). As the differentiation continues, the filaggrin monomers are processed to hygroscopic amino acids and these breakdown products function as moisturizing factors (Palmer et al., 2006). We show that TAM67-expressing embryonic epidermis displays markedly reduced profilaggrin mRNA level, and filaggrin and profilaggrin protein content, and reduced keratohyalin granule number. Thus, AP1 factor loss, leading to reduced profilaggrin and filaggrin content, may explain many features of the phenotype, as filaggrin loss is observed in the flaky tail mouse (a model of ichthyosis vulgaris) and is a feature of human ichthyosis vulgaris (Presland et al., 2000; McLean, 2016; Smith et al., 2006; Oji and Traupe, 2006; Oji and Traupe, 2009; Gruber et al., 2011).

Collodion membrane phenotype However, it is not clear that filaggrin loss can explain the formation of the collodion membrane in newborn mouse embryos, since filaggrin loss is not associated with a collodion phenotype in the flaky tail mouse ichthyosis vulgaris model (Presland et al., 2000; Smith et al., 2006) or in ichthyosis vulgaris patients (McLean, 2016). Moreover, in lamellar ichthyosis, where collodion membrane formation is common, filaggrin is present at elevated levels (Rice et al., 2013; Paller et al., 2016). Although we cannot assign a definitive cause for the collodion phenotype in TAM67-expressing AP1 factor-deficient epidermis, we speculate that this may be a response to a change in loricrin distribution. Loricrin is an abundant epidermal cornified envelope precursor protein (Candi et al., 2005; Mehrel et al., 1990; Hohl et al., 1991; Mehrel et al., 1990) and a frameshift mutation adds a nuclear localization signal to the loricrin c-terminus (Korge et al., 1997; Maestrini et al., 1996; O'Driscoll et al., 2002; Matsumoto et al., 2001; Takahashi et al., 1999; Gedicke et al., 2006; Drera et al., 2008) which leads to its nuclear accumulation in keratinocytes in loricrin keratoderma patients (Ishida-Yamamoto et al., 1998; Ishida-Yamamoto, 2003). Loricrin keratoderma is a form of ichthyosis that is associated with a collodion phenotype in 36% of newborns (Yeh et al., 2013).

Although the mechanism is not well understood, there are several ideas about how nuclear loricrin may impact the epidermis. It is possible that nuclear loricrin accumulation reduces loricrin content at the cell periphery and thereby impairs cornified envelope assembly and that this leads to compromised barrier function and collodion phenotype. It is also possible that nuclear loricrin alters keratinocyte gene expression to impair cell viability or alter epidermal differentiation or apoptosis. Consistent with such a role, we observe a marked shift of loricrin from the cytoplasmic to nuclear compartment in AP1 factor inactivated epidermis of E13.5, E15.5 and E17.5 mice and in cultured cells derived from these mice. This fits with our previous findings showing nuclear loricrin localization in the epidermis of adult TAM67-expressing epidermis (Rorke et al., 2015a; Rorke et al., 2015b). It is interesting that wild-type loricrin moves to the nucleus in the epidermal cells of these AP1

factor perturbed mice (Rorke et al., 2015a; Rorke et al., 2015b). This is in contrast to loricrin keratoderma, where a frame-shift mutation creates a nuclear localization signal that moves loricrin to the nucleus (Korge et al., 1997; Maestrini et al., 1996; O'Driscoll et al., 2002; Matsumoto et al., 2001; Takahashi et al., 1999; Gedicke et al., 2006; Drera et al., 2008).

However, the causes of the collodion phenotype are likely to be complex, as other forms of ichthyosis, such as lamellar ichthyosis and congenital ichthyosiform erythroderma, manifest a collodion baby phenotype (Oji et al., 2010), but nuclear loricrin accumulation has not been reported in these diseases. In addition, other underlying causes are associated with collodion phenotype. For example, a collodion phenotype is frequently observed in ichthyosis patients harboring mutations in the transglutaminase 1 gene (Oji et al., 2010; Farasat et al., 2009). Our studies demonstrate a role for AP1 factors in maintaining normal epidermal function during embryogenesis, and indicate that loss of AP1 factor function can cause a phenotype that manifests ichthyotic features. These studies also attest to the complex responses that can be observed when perturbing a single class of transcription regulators in epidermis. Moreover, the timing of AP1 factor inactivation during epidermal differentiation appears to be important. Although we observe a dramatic phenotype when AP1 factor function is inactivated in the suprabasal layers, no phenotype is observed following basal layer AP1 factor inactivation (Young et al., 1999). Further study will be necessary to determine whether AP1 factors loss has a role in the pathogenesis of human ichthyoses and to understand how AP1 factor deficiency drives the collodion membrane phenotype.

Materials and Methods

Embryo Studies

Construction of the TAM67-rTA transgenic mouse was previously described (Rorke et al., 2010). These mice encode a doxycycline-inducible cassette encoding TAM67, a dominant-negative form of c-jun that inhibits function of all AP1 factors (Rorke et al., 2010). Induction of TAM67 expression results in an ichthyosis/keratoderma-like phenotype (Rorke et al., 2010). To study the role of AP1 factor inactivation in embryonic epidermis, we mated heterozygous (TAM67+/−) and heterozygous (rTA+/−) mice and treated the pregnant dams with doxycycline (2 mg/ml) in drinking water beginning on embryonic days E13.5, E15.5, and E17.5. At E20, prior to birth, the pups were euthanized and harvested. We use the SKH1 hairless mouse genetic background so that epidermal phenotypes can be readily visualized (Rorke et al., 2010; Rorke et al., 2015b). The SKH1 hairless mice are immune competent (Benavides et al., 2009). Dorsal total skin was removed, sections were prepared for histology and the remaining skin was flash frozen in liquid nitrogen, powdered and stored at −80 C. These studies were approved by the Institutional Animal Care and Use Committee and followed the NIH Guidelines for the Care and Use of Laboratory Animals. Statistical analysis was performed using the student’s t-test.

Skin permeability assay

Pups were removed from the womb at E20, euthanized, rinsed in phosphate-buffered saline (PBS), immersed sequentially in 25%, 50%, 75% and 100% methanol (1 min each), PBS, 0.1% toluidine blue for 6 – 8 min, and then rinsed in PBS and photographed.

Cornified envelope images and quantification

An 8 mm punch biopsy of dorsal embryonic skin was collected and the whole tissue (epidermis and dermis) was boiled for 20 min in 20 mM Tris-HCl (pH 7.5), 5 mM EDTA, 10 mM DTT, and 2% sodium dodecyl sulfate. Cornified envelopes were collected by centrifugation and counted using a hemocytometer. Data is graphed as average cornified envelope number/5 μl volume.

Filaggrin mRNA

Filaggrin and filaggrin 2 mRNA level was measured by treating pregnant dams with 2 mg/ml doxycycline in drinking water beginning at E13.5, E15.5 and E17.5. The pups were excised at E20 and whole skin was flash frozen, pulverized and RNA was converted to cDNA followed by qRT-PCR detection of filaggrin and filaggrin 2 mRNA (Chew et al., 2011). Filaggrin primer set 1 (P1): 5’-GAA TCC ATA TTT ACA GCA AAG CAC CTT G and 5’-GGT ATG TCC AAT GTG ATT GCA CGA TTG. Filaggrin primer set 2 (P2): 5’-GAA GGA ACT TCT GGA AGG ACA AC and 5’-TCC ATC AGT TCC ACC ATG CCT C (Presland et al., 2000; Hansmann et al., 2012). Filaggrin 2 primers set: 5’-GAG CAA GGA TGA GCT AAA GGA AC and 5’-GCC ACG CCT ATG CTT CTT TGA C (Presland et al., 2000; Hansmann et al., 2012).

Immunological methods

Immunofluorescence was performed using paraffin-embedded formalin-fixed sections (Rorke et al., 2010). Anti-loricrin (PRB-145P), anti-K14 (PRB-155P), anti-K10 (PRB-159P) and anti-Filaggrin (PRB-417P) were form Covance (Emeryville, CA). Anti-FLAG (M2) and anti-β-actin (A-5441) were from Sigma (St. Louis, MO), and anti-PCNA (sc-56) was from Santa Cruz (Dallas, TX). Anti-involucrin was prepared in our laboratory. Primary antibody binding was detected using Cy3-conjugated goat anti-rat IgG (A10522) or Alexafluor 488-conjugated goat anti-rabbit IgG (A11034) from Invitrogen (Waltham, MA).

Immunoblot extracts were prepared from flash frozen/powdered skin (epidermis + dermis) by dissolving in lysis buffer containing 0.625 M Tris-HCl, pH 7.5, 10% glycerol, 5% SDS, 5% β-mercaptoethanol. Equal amounts of protein were electrophoresed on 12% denaturing polyacrylamide gels.

Cell culture

Total skin was harvested from newborn TAM67-negative and -positive pups and incubated overnight in 5 mg/ml dispase at 4°C. Epidermis was separated from the dermis and incubated in 0.25% trypsin at 37°C for 15 min. Incubation was stopped by adding soybean trypsin inhibitor to 0.5 mg/ml, and the cells were strained through a 100 μm nylon strainer and centrifuged at 2,000 rpm for 5 min. Cells were resuspended in low calcium (0.05 mM) Keratinocyte serum-free medium and plated at 79,000 cells per cm^2 in type I rat collagen-coated 100 mm culture dishes (Cultrex type I rat tail collagen, R&D Systems, 3440-100-01, Minneapolis, MN). The cells were fed every other day, and doxycycline was added at 1 μg/ml to induce TAM67-FLAG expression.

Electron microscopy

Embryonic skin biopsies were taken for electron microscopy (Hou et al., 1991). Briefly, samples were minced to < 0.5 mm^3, fixed in modified Karnovsky's fixative overnight, postfixed in 1% aqueous osmium tetroxide containing 1.5% potassium ferrocyanide or in 0.2% ruthenium tetroxide (the latter only where indicated in figure legends). The samples were dehydrated in a graded ethanol series and embedded in an Epon-epoxy mixture. Ultrathin sections were examined, with or without further contrasting with lead citrate, in a JEOL electron microscope (JEOL USA, Inc, Peabody, MA, USA).

Gene array analysis

For gene array analysis, we mated heterozygous (TAM67+/−) and heterozygous (rTA+/−) mice and treated the pregnant dams with doxycycline (2 mg/ml) in drinking water beginning on embryonic days E15.5. At E20 the pups were euthanized and RNA was collected from whole skin. RNA samples were pooled using epidermis from three separate mice. Approximately 5 to 8 μg of total RNA was reverse transcribed, amplified and labeled as described (Li et al., 2001) and labeled cRNAs were hybridized to Affymetrix Mouse Gene 1.0 ST Arrays (#901168) and 0.5 fold or greater change in expression was considered significant. For annotation we used the DAVID program [http://david.abcc.ncifcrf.gov] (Dennis et al., 2003).

Acknowledgments

This work was supported by National Institutes of Health grants to RLE (AR065266, CA131074 and CA184027).

Abbreviations

CE	cornified envelope
AP1	activator protein 1

References

Angel P, Szabowski A, Schorpp-Kistner M. Function and regulation of AP-1 subunits in skin physiology and pathology. Oncogene. 2001; 20:2413–23. [PubMed: 11402337]

Benavides F, Oberyszyn TM, VanBuskirk AM, Reeve VE, Kusewitt DF. The hairless mouse in skin research. J Dermatol Sci. 2009; 53:10–8. [PubMed: 18938063]

Candi E, Schmidt R, Melino G. The cornified envelope: a model of cell death in the skin. Nat Rev Mol Cell Biol. 2005; 6:328–40. [PubMed: 15803139]

Chew YC, Adhikary G, Wilson GM, Reece EA, Eckert RL. PKCdelta suppresses keratinocyte proliferation by increasing p21CIP1 level by a KLF4-dependent mechanism. J Biol Chem. 2011; 286:28771–82.

Crish JF, Gopalakrishnan R, Bone F, Gilliam AC, Eckert RL. The distal and proximal regulatory regions of the involucrin gene promoter have distinct functions and are required for in vivo involucrin expression. J Invest Dermatol. 2006; 126:305–14. [PubMed: 16374477]

Crish JF, Zaim TM, Eckert RL. The distal regulatory region of the human involucrin promoter is required for expression in epidermis. J Biol Chem. 1998; 273:30460–5. [PubMed: 9804813]

Dale BA, Resing KA, Lonsdale-Eccles JD. Filaggrin: a keratin filament associated protein. Ann N Y Acad Sci. 1985; 455:330–42. [PubMed: 2417519]

Dennis G, Sherman BT, Hosack DA, Yang J, Gao W, Lane HC, et al. DAVID: Database for Annotation, Visualization, and Integrated Discovery. Genome Biol. 2003; 4:3.

Drera B, Tadini G, Balbo F, Marchese L, Barlati S, Colombi M. De novo occurrence of the 730insG recurrent mutation in an Italian family with the ichthyotic variant of Vohwinkel syndrome, loricrin keratoderma. Clin Genet. 2008; 73:85–8. [PubMed: 17953701]

Eckert RL, Crish JF, Banks EB, Welter JF. The epidermis: genes on - genes off. J Invest Dermatol. 1997; 109:501–9. [PubMed: 9326381]

Farasat S, Wei MH, Herman M, Liewehr DJ, Steinberg SM, Bale SJ, et al. Novel transglutaminase-1 mutations and genotype-phenotype investigations of 104 patients with autosomal recessive congenital ichthyosis in the USA. J Med Genet. 2009; 46:103–11. [PubMed: 18948357]

Gedicke MM, Traupe H, Fischer B, Tinschert S, Hennies HC. Towards characterization of palmoplantar keratoderma caused by gain-of-function mutation in loricrin: analysis of a family and review of the literature. Br J Dermatol. 2006; 154:167–71. [PubMed: 16403113]

Gruber R, Elias PM, Crumrine D, Lin TK, Brandner JM, Hachem JP, et al. Filaggrin genotype in ichthyosis vulgaris predicts abnormalities in epidermal structure and function. Am J Pathol. 2011; 178:2252–63. [PubMed: 21514438]

Hansmann B, Ahrens K, Wu Z, Proksch E, Meyer-Hoffert U, Schroder JM. Murine filaggrin-2 is involved in epithelial barrier function and down-regulated in metabolically induced skin barrier dysfunction. Exp Dermatol. 2012; 21:271–6. [PubMed: 22417302]

Hohl D, Mehrel T, Lichti U, Turner ML, Roop DR, Steinert PM. Characterization of human loricrin. Structure and function of a new class of epidermal cell envelope proteins. J Biol Chem. 1991; 266:6626–36. [PubMed: 2007607]

Hou SY, Mitra AK, White SH, Menon GK, Ghadially R, Elias PM. Membrane structures in normal and essential fatty acid-deficient stratum corneum: characterization by ruthenium tetroxide staining and x-ray diffraction. J Invest Dermatol. 1991; 96:215–23. [PubMed: 1991982]

Irvine AD. Fleshing out filaggrin phenotypes. J Invest Dermatol. 2007; 127:504–7. [PubMed: 17299430]

Irvine AD, McLean WH, Leung DY. Filaggrin mutations associated with skin and allergic diseases. N Engl J Med. 2011; 365:1315–27. [PubMed: 21991953]

Ishida-Yamamoto A. Loricrin keratoderma: a novel disease entity characterized by nuclear accumulation of mutant loricrin. J Dermatol Sci. 2003; 31:3–8. [PubMed: 12615358]

Ishida-Yamamoto A, Takahashi H, Iizuka H. Loricrin and human skin diseases: molecular basis of loricrin keratodermas. Histol Histopathol. 1998; 13:819–26. [PubMed: 9690138]

Ishida-Yamamoto A, Tanaka H, Nakane H, Takahashi H, Hashimoto Y, Iizuka H. Programmed cell death in normal epidermis and loricrin keratoderma. Multiple functions of profilaggrin in keratinization. J Investig Dermatol Symp Proc. 1999; 4:145–9.

Jang SI, Steinert PM, Markova NG. Activator protein 1 activity is involved in the regulation of the cell type-specific expression from the proximal promoter of the human profilaggrin gene. J Biol Chem. 1996; 271:24105–14. [PubMed: 8798649]

Korge BP, Ishida-Yamamoto A, Punter C, Dopping-Hepenstal PJ, Iizuka H, Stephenson A, et al. Loricrin mutation in Vohwinkel's keratoderma is unique to the variant with ichthyosis. J Invest Dermatol. 1997; 109:604–10. [PubMed: 9326398]

Li D, Turi TG, Schuck A, Freedberg IM, Khitrov G, Blumenberg M. Rays and arrays: the transcriptional program in the response of human epidermal keratinocytes to UVB illumination. FASEB J. 2001; 15:2533–5. [PubMed: 11641260]

Maestrini E, Monaco AP, McGrath JA, Ishida Yamamoto A, Camisa C, Hovnanian A, et al. A molecular defect in loricrin, the major component of the cornified cell envelope, underlies Vohwinkel's syndrome. Nat Genet. 1996; 13:70–7. [PubMed: 8673107]

Matsumoto K, Muto M, Seki S, Saida T, Horiuchi N, Takahashi H, et al. Loricrin keratoderma: a cause of congenital ichthyosiform erythroderma and collodion baby. Br J Dermatol. 2001; 145:657–60. [PubMed: 11703298]

McLean WH. Filaggrin failure - from ichthyosis vulgaris to atopic eczema and beyond. Br J Dermatol. 2016; 175(Suppl 2):4–7.

Mehrel T, Hohl D, Rothnagel JA, Longley MA, Bundman D, Cheng C, et al. Identification of a major keratinocyte cell envelope protein, loricrin. J Cell Biochem. 1990; 61:1103–12.

O'Driscoll J, Muston GC, McGrath JA, Lam HM, Ashworth J, Christiano AM. A recurrent mutation in the loricrin gene underlies the ichthyotic variant of Vohwinkel syndrome. Clin Exp Dermatol. 2002; 27:243–6. [PubMed: 12072018]

Oji V, Tadini G, Akiyama M, Blanchet BC, Bodemer C, Bourrat E, et al. Revised nomenclature and classification of inherited ichthyoses: results of the First Ichthyosis Consensus Conference in Soreze 2009. J Am Acad Dermatol. 2010; 63:607–41. [PubMed: 20643494]

Oji V, Traupe H. Ichthyoses: differential diagnosis and molecular genetics. Eur J Dermatol. 2006; 16:349–59. [PubMed: 16935789]

Oji V, Traupe H. Ichthyosis: clinical manifestations and practical treatment options. Am J Clin Dermatol. 2009; 10:351–64. [PubMed: 19824737]

Paller AS, Renert-Yuval Y, Suprun M, Esaki H, Oliva M, Huynh TN, et al. An IL-17-dominant immune profile is shared across the major orphan forms of ichthyosis. J Allergy Clin Immunol. 2016

Palmer CN, Irvine AD, Terron-Kwiatkowski A, Zhao Y, Liao H, Lee SP, et al. Common loss-of-function variants of the epidermal barrier protein filaggrin are a major predisposing factor for atopic dermatitis. Nat Genet. 2006; 38:441–6. [PubMed: 16550169]

Presland RB, Boggess D, Lewis SP, Hull C, Fleckman P, Sundberg JP. Loss of normal profilaggrin and filaggrin in flaky tail (ft/ft) mice: an animal model for the filaggrin-deficient skin disease ichthyosis vulgaris. J Invest Dermatol. 2000; 115:1072–81. [PubMed: 11121144]

Rice RH, Bradshaw KM, Durbin-Johnson BP, Rocke DM, Eigenheer RA, Phinney BS, et al. Distinguishing ichthyoses by protein profiling. PLoS One. 2013; 8:e75355. [PubMed: 24130705]

Robinson NA, LaCelle PT, Eckert RL. Involucrin is a covalently crosslinked constituent of highly purified epidermal corneocytes: evidence for a common pattern of involucrin crosslinking in vivo and in vitro. J Invest Dermatol. 1996; 107:101–7. [PubMed: 8752847]

Robinson NA, Lapic S, Welter JF, Eckert RL. S100A11, S100A10, annexin I, desmosomal proteins, small proline-rich proteins, plasminogen activator inhibitor-2, and involucrin are components of the cornified envelope of cultured human epidermal keratinocytes. J Biol Chem. 1997; 272:12035–46. [PubMed: 9115270]

Rorke EA, Adhikary G, Jans R, Crish JF, Eckert RL. AP1 factor inactivation in the suprabasal epidermis causes increased epidermal hyperproliferation and hyperkeratosis but reduced carcinogen-dependent tumor formation. Oncogene. 2010; 29:5873–82. [PubMed: 20818430]

Rorke EA, Adhikary G, Young CA, Rice RH, Elias PM, Crumrine D, et al. Structural and biochemical changes underlying a keratoderma-like phenotype in mice lacking suprabasal AP1 transcription factor function. Cell Death Dis. 2015a; 6:e1647. [PubMed: 25695600]

Rorke EA, Adhikary G, Young CA, Roop DR, Eckert RL. Suppressing AP1 factor signaling in the suprabasal epidermis produces a keratoderma phenotype. J Invest Dermatol. 2015b; 135:170–80. [PubMed: 25050598]

Sandilands A, Sutherland C, Irvine AD, McLean WH. Filaggrin in the frontline: role in skin barrier function and disease. J Cell Sci. 2009; 122:1285–94. [PubMed: 19386895]

Smith FJ, Irvine AD, Terron-Kwiatkowski A, Sandilands A, Campbell LE, Zhao Y, et al. Loss-of-function mutations in the gene encoding filaggrin cause ichthyosis vulgaris. Nat Genet. 2006; 38:337–42. [PubMed: 16444271]

Takahashi H, Ishida-Yamamoto A, Kishi A, Ohara K, Iizuka H. Loricrin gene mutation in a Japanese patient of Vohwinkel's syndrome. J Dermatol Sci. 1999; 19:44–7. [PubMed: 9890374]

Welter JF, Eckert RL. Differential expression of fos and jun family members c-fos, fosB, Fra-1, Fra-2, c-jun, junB and junD during human epidermal keratinocyte differentiation. Oncogene. 1995; 11:2681–7. [PubMed: 8545126]

Yeh JM, Yang MH, Chao SC. Collodion baby and loricrin keratoderma: a case report and mutation analysis. Clin Exp Dermatol. 2013; 38:147–50. [PubMed: 22831754]

Young MR, Li JJ, Rincon M, Flavell RA, Sathyanarayana BK, Hunziker R, et al. Transgenic mice demonstrate AP-1 (activator protein-1) transactivation is required for tumor promotion. Proc Natl Acad Sci U S A. 1999; 96:9827–32. [PubMed: 10449779]

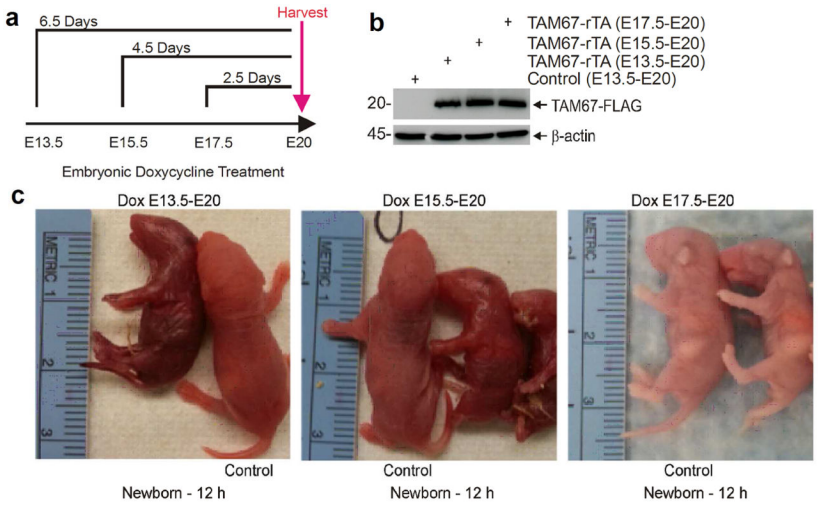

Fig. 1. AP1 factor inactivation in epidermis produces a collodion baby-like phenotype

A We mated heterozygous (TAM67+/−) and heterozygous (rTA+/−) mice and the pregnant dams were treated with 2 mg/ml doxycycline in drinking water beginning on E13.5, E15.5 and E17.5. The embryos were collected on E20 or as newborns. **B** Skin extracts were prepared from individual embryos following treatment as indicated in panel A and TAM67-FLAG levels were assayed in extracts from E20 embryos by anti-FLAG immunoblot. **C** Pregnant dams were treated with doxycycline as indicated in each panel and the phenotype of each newborn mouse was photographed at 12 h after birth. The mice are TAM67-positive except for those labeled control.

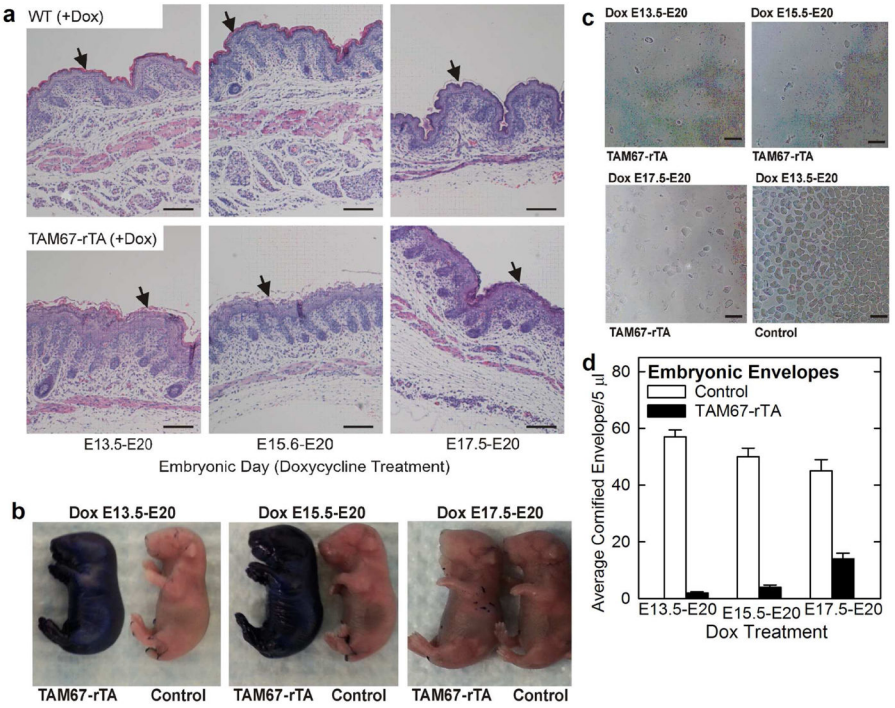

Fig. 2. Impact of AP1 factor inactivation on epidermal structure and barrier function

A H&E stained sections of embryonic epidermis were prepared from individual E20 embryos following treatment as indicated in Fig. 1A. The arrows denote cornified layer. The bar = 100 microns. **B** Embryos were collected at E20 and stained with 0.1% toluidine blue to assess skin permeability. **C/D** Epidermis was harvested from embryos at E20 and boiled in denaturing/reducing buffer prior to cornified envelope counting. Bars = 100 microns. The values are mean ± SEM, n = 4. TAM67-rTA values are significantly reduced as compared to control ($p < 0.001$).

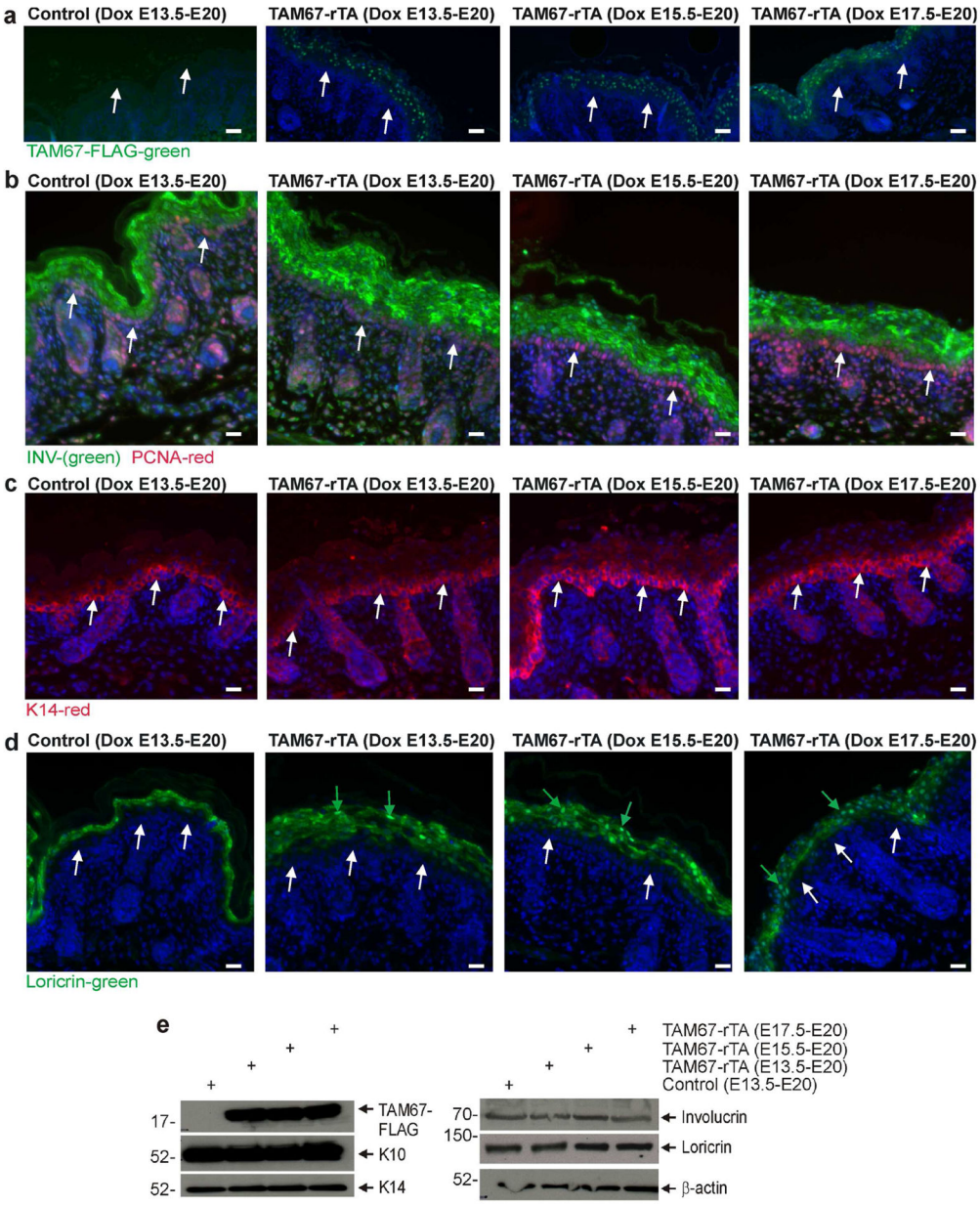

Fig. 3. Distribution of differentiation markers in TAM67-positive embryonic epidermis

A/B/C/D Pregnant dams were treated with 2 mg/ml doxycycline on E13.5-E20, E15.5-E20 or E17.5-E20 and the embryos were harvested on E20 and the epidermis sectioned. Sections were stained to detect the indicated epitopes and also DAPI stained to detect the nuclei. The white arrows indicate the epidermal basal layer and green arrows indicate nuclear loricrin. **E** Following treatment of the dams with doxycycline as indicated, whole skin (dermis/epidermis) extracts were prepared from E20 embryos for immunoblot. Similar findings were observed in each of three replicate experiments.

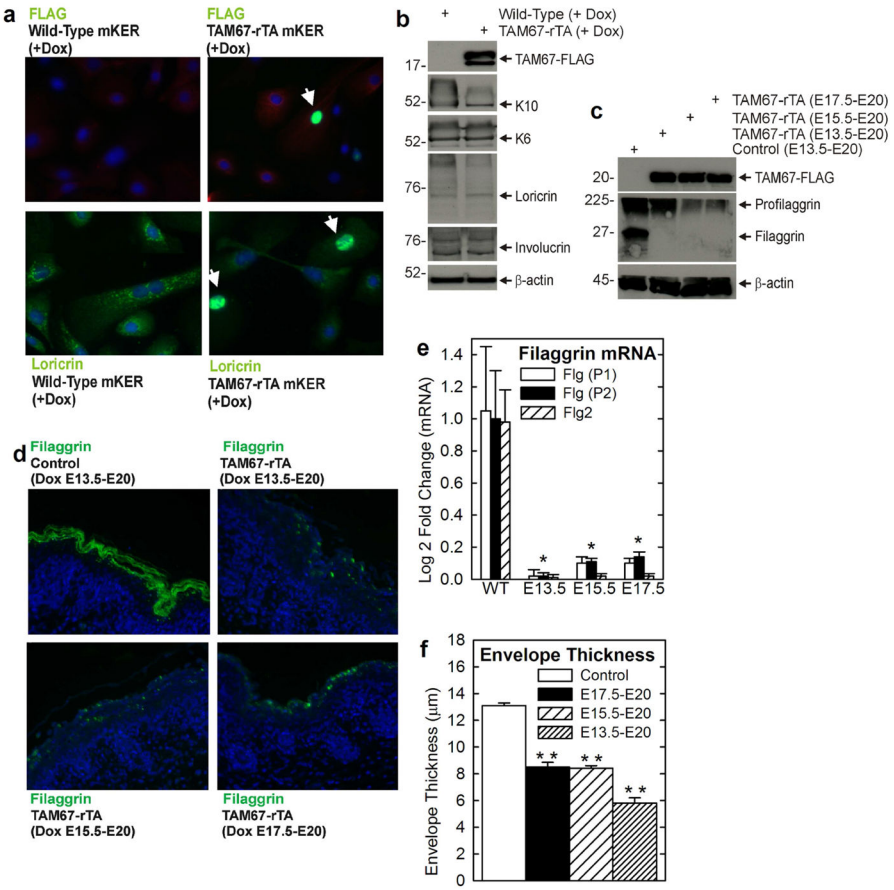

Fig. 4. AP1 factor loss regulates loricrin distribution and filaggrin level

A/B Murine keratinocytes were harvested from newborn mice and wild-type and TAM67-positive cells were grown as monolayer cultures and treated with 1 μg/ml doxycycline for 8 d. The cells were then fixed and stained to detect TAM67-FLAG (anti-FLAG) and loricrin. The arrows indicate nuclear localization of the TAM67-FLAG (top panels) and loricrin (bottom panels). Extracts were prepared from the above cells after doxycycline treatment for 8 d followed by immunoblot detection of the indicated proteins. Similar results were observed in each of three replicate experiments. **C/D/E** Suprabasal epidermal TAM67 expression is associated with reduced profilaggrin and filaggrin levels. Pregnant dams were treated with 2 mg/ml doxycycline in drinking water on E13.5, E15.5 and E17.5 of embryo development and embryos were harvested at E20. Sections were collected and stained with anti-filaggrin to detect filaggrin distribution in the embryonic epidermis. Similar results were observed in each of four independent experiments. Whole skin extracts were collected for immunoblot detection of TAM67-FLAG (anti-FLAG) and profilaggrin/filaggrin (anti-filaggrin), and qRT-PCR detection of filaggrin and filaggrin 2 mRNA. The graph values are mean ± SEM, n = 3. The asterisks indicate a significant reduction in mRNA (compared to WT) as assessed using the student's t-test ($p < 0.001$). **F** Cornified envelope thickness is reduced in TAM67-positive epidermis. EM images were measured for cornified envelope thickness. The values (μm) are mean ± SEM, n = 20, $p < 0.0001$. All cornified envelope thickness measurements were made in the granular layer.

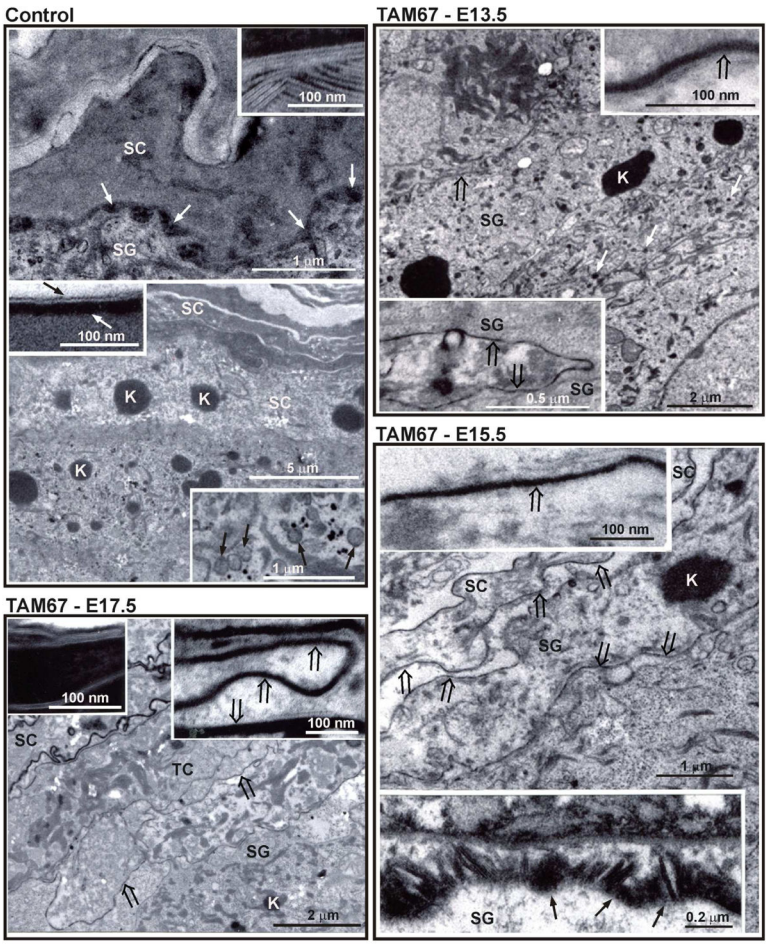

Fig. 5. Ultrastructure of TAM67-positive embryonic epidermis

Pregnant dams were treated with 2 mg/ml doxycycline beginning at E13.5, E15.5 and E17.5 and at E20 embryonic whole skin punch biopsies were harvested for ultrastructural characterization. Wild-type control embryos include TAM67-/rTA−, TAM67+/rTA− and TAM67-/rTA+ genotypes. Images from control epidermis show robust secretion of granular contents at the SG-SC junction (white arrows, upper panel), abundant keratohyalin granules (K, lower panel), extensive membrane arrays formed from processing of secreted lipids (top insert), formation of thick, well-formed cornified envelopes (middle insert, flanked by black and white arrows), and the presence of normal and abundant lamellar bodies in the SG (black arrows, bottom insert). In contrast, envelope thickness is reduced in E13.5, E15.5 and E17.5 mouse epidermis (black double arrows) and keratohyalin granule size and number are reduced (K). The solid white arrows in the E13.5 panel indicate lamellar bodies which appear normal and are present at normal numbers. In the E15.5 panel, the solid black arrows show defective secretion of granular contents at the SG-SC interface (lower insert). The left insert in the E17.5 panel indicates an enlarged view of the cornified layer. Abbreviations: SC, stratum corneum; TC, transition cells; SG, stratum granulosum; K, keratohyalin granules. The upper right insert in control, and the upper left insert in E17.5 were stained with ruthenium tetroxide.

Table 1

Gene array analysis

Ratio: (log2)[a] *TAM67+/TAM67−*	Gene Name	Entrez Gene ID	Description	Category
Gene expression elevated in TAM67-negative epidermis				
−1.98	*Krt23*	94179	Keratin 23	Cutaneous keratins
−0.62	*Krt7*	110310	Keratin 7	
−0.73	*Krt13*	16663	Keratin 13	
−0.87	*Krt4*	794486	Keratin 4	
−1.10	*Krt78*	332131	Keratin 78	
−0.60	*Krt84*	16680	Keratin 84	Hair keratins
−0.74	*Krt36*	16673	Keratin 36	
−0.66	*Krtap5-1*	50774	Keratin associated protein 5-1	
−0.97	*Gm10272*	16697	Keratin associated protein 12-4	
−2.66	*Kprp*	433619	Keratinocyte expressed proline-rich	
−3.66	*Lce1m*	66203	Late cornified envelope 1m	Late envelope
−3.17	*Lce1b*	68720	Late cornified envelope 1b	
−2.94	*Lce1c*	73719	Late cornified envelope 1c	
−2.22	*Lce1j*	545547	Late cornified envelope 1j	
−1.42	*Lce1f*	67828	Late cornified envelope 1f	
−1.07	*Lce1d*	69611	Late cornified envelope 1d	
−1.46	*Lor*	16939	Loricrin	
−3.39	*Flg2*	229574	Filaggrin family member 2	Filaggrin related
−1.64	*Hrnr*	68723	Hornerin	
Gene expression elevated in TAM67-positive epidermis				
+4.46	*Krt16*	16666	Keratin 16 (proliferation-associated)	Cutaneous keratins
+2.10	*Krt6b*	16688	Keratin 6b (proliferation-associated)	
+1.40	*Krt6a*	16687	Keratin 6a (proliferation-associated)	
+2.89	*Sprr1b*	20754	Small proline rich protein 1b	Early envelope
+0.74	*Sprr1a*	20753	Small protein rich protein 1a	
+0.74	*Prr29*	75573	Proline rich 29	
+0.71	*Prrg4*	228413	Proline rich G-carboxyglutamic acid 4	
+0.99	*Serpin b11*	66957	Serine (or cysteine) peptidase inhibitor,	Proteases and
+0.93	*Lyz2*	17105	Lysozyme 2	
+0.81	*Klk1b4*	18048	Kallikrein 1-related peptidase b4	
+0.71	*Cela3a*	242711	Chymotrypsin-like elastase family member	
+0.70	*Cts3*	117066	Cathepsin 3	
+0.68	*Serpinb6c*	97848	Serine (or cysteine) peptidase inhibitor, clade B, member 6c	
+1.31	*Defa21*	66298	Defensin α21	Envelope defense
+0.94	*Defa-rs2*	13222	Defensin alpha-related sequence 2	

Ratio: (log2)[a] *TAM67+/TAM67−*	**Gene Name**	**Entrez Gene ID**	**Description**	**Category**
+0.73	*Defa29*	13218	Defensin alpha 29	
+0.69	*Defb7*	246080	Defensin beta 7	
+1.31	*Defa21*	66298	Defensin α21	
+2.35	*Rptn*	20129	Repetin	Filaggrin related

[a]Negative log2 values indicate relative enrichment in TAM67-negative skin and positive numbers indicate relative enrichment in TAM67-positive skin.